Feature-tracking computed tomography left atrial strain and long-term survival after transcatheter aortic valve implantation

Hirasawa, K.; Singh, G.K.; Kuneman, J.H.; Gegenava, T.; Kley, F. van der; Hautemann, D.; ... ; Delgado, V.

ESC European Society of Cardiology

European Heart Journal - Cardiovascular Imaging (2023) **24**, 327–335
https://doi.org/10.1093/ehjci/jeac157

ORIGINAL PAPER

Feature-tracking computed tomography left atrial strain and long-term survival after transcatheter aortic valve implantation

Kensuke Hirasawa [1], Gurpreet K. Singh[1], Jurrien H. Kuneman [1], Tea Gegenava [1], Frank van der Kley [1], David Hautemann[2], Johan H.C. Reiber [3,4], Nina Ajmone Marsan [1], Jeroen J. Bax [1,5], and Victoria Delgado [1,6]*

[1]Department of Cardiology, Heart Lung Centre, Leiden University Medical Center, Albinusdreef 2, 2333 ZA Leiden, The Netherlands; [2]TestDynamics EU B.V, 2665 CZ Bleiswijk, The Netherlands; [3]Medis Medical Imaging BV, 2316 XG Leiden, The Netherlands; [4]LKEB, Leiden University Medical Center, 2333 ZA Leiden, The Netherlands; [5]Heart Center, University of Turku and Turku University Hospital, 20521 Turku, Finland; and [6]Heart Institute, Hospital University Germans Trias i Pujol, 08916 Badalona, Spain

Received 11 March 2022; editorial decision 26 July 2022; accepted 27 July 2022; online publish-ahead-of-print 12 August 2022

Aims Aortic stenosis (AS) induces left atrial (LA) remodelling through the increase of left ventricular (LV) filling pressures. Peak LA longitudinal strain (PALS), reflecting LA reservoir function, has been proposed as a prognostic marker in patients with AS. Feature-tracking (FT) multi-detector computed tomography (MDCT) allows assessment of LA strain from MDCT data. The aim of this study is to investigate the association between PALS using FT MDCT and survival in patients with severe AS who underwent transcatheter aortic valve implantation (TAVI).

Methods and results A total of 376 patients (mean age 80 ± 7 years, 53% male) who underwent MDCT before TAVI and had suitable data for assessment of PALS using dedicated FT software, were included. The patients were classified into four groups according to PALS quartiles; PALS > 19.3% (Q1, highest reservoir function), 15.0–19.3% (Q2), 9.1–14.9% (Q3), and ≤9.0% (Q4, lowest reservoir function). The primary outcome was all-cause mortality. During a median of 45 (22–68) months follow-up, 148 patients (39%) died. On multivariable Cox regression analysis, PALS was independently associated with all-cause mortality [hazard ratio (HR): 1.044, 95% confidence interval (CI): 1.012–1.076, $P = 0.006$]. Compared with patients in Q1, patients in Q3 and Q4 were associated with higher risk of mortality after TAVI [HR: 2.262 (95% CI: 1.335–3.832), $P = 0.002$ for Q3, HR: 3.116 (95% CI: 1.864–5.210), $P < 0.001$ for Q4].

Conclusion PALS assessed with FT MDCT is independently associated with all-cause mortality after TAVI.

* Corresponding author. Tel: +31 715262020; Fax: +31 715266809. E-mail: v.delgado@lumc.nl

Graphical Abstract

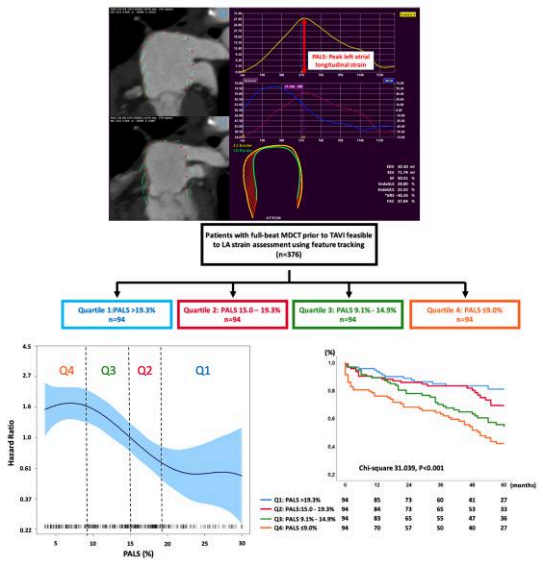

Feature-tracking computed tomography assessment of left atrial reservoir strain in patients with severe aortic stenosis treated with transcatheter aortic valve implantation.

Keywords computed tomography • transcatheter aortic valve implantation • aortic stenosis • left atrium • left atrial strain

Introduction

The left atrium (LA) plays an important role as a reservoir, modulating left ventricular (LV) filling. In addition, the assessment of peak LA longitudinal strain (PALS), which reflects the LA reservoir function, has shown incremental prognostic value over LA size in various cardiac diseases,[1–4] including severe aortic stenosis (AS).[5–7] Two-dimensional (2D) speckle tracking echocardiography (STE) is frequently used to measure PALS from echocardiographic data. More recently, feature tracking (FT) applied to multi-detector row computed tomography (MDCT) data permits the assessment of PALS when the data are acquired throughout the entire cardiac cycle and have shown good agreement with echocardiographic speckle tracking-derived PALS.[8,9] MDCT is a key imaging tool for planning transcatheter aortic valve implantation (TAVI) in patients with severe AS who are not candidates for surgical aortic valve replacement. Aortic annulus size and calibre, calcification and tortuosity of the femoral, and iliac arteries are the main parameters to select the prosthesis size and the TAVI access route. Furthermore, there are several additional parameters that have been associated with outcomes after TAVI such as calcification of the thoracic aorta[10] and LV global longitudinal strain (LV GLS).[11,12] However, the utility of PALS assessment using FT MDCT for patients with severe AS treated with TAVI has not been investigated. The feasibility and reproducibility of PALS measured by MDCT in patients with sinus rhythm and atrial fibrillation have been reported.[9] However the association between PALS measured with FT-MDCT and outcomes in patients treated with TAVI have not been investigated. Accordingly, this study aimed to investigate the association between PALS measured with FT MDCT and survival in patients with severe AS treated with TAVI.

Methods

Study population and clinical data collection

Patients with severe AS referred for TAVI and who had pre-procedural full-beat MDCT data at the Leiden University Medical Center, The Netherlands, were included in the current retrospective analysis. Patients with insufficient MDCT data for FT strain analysis were excluded. Patients were classified into four groups according to the PALS quartiles to compare the survival rates after TAVI (*Figure 1*). All clinical data including demographics, cardiovascular risk factors, medication, and New York Heart Association (NYHA) functional class symptoms at baseline (before TAVI) were collected from the medical records of the cardiology department (EPD vision version 12.5.4; Leiden, The Netherlands). The institutional review board approved this retrospective analysis of clinically acquired data and the need for patient written informed consent was waived.

MDCT data acquisition and assessment

MDCT scans were performed before TAVI using a 64-slice ($n = 18$, Aquilion64, Toshiba Medical Systems, Otawara, Japan) or a 320-slice CT scanner ($n = 358$, AquilionOne, Toshiba Medical Systems, Tochigi-ken, Japan): 120 kV, 300 mA, a rotation time of 400–500 ms (depending on the heart rate), and collimation of 64 × 0.5 mm for 64-slice CT scanner; and 100–120 kV, 400–580 mA with a minimum rotation time of 350 ms, and collimation of 320 × 0.5 mm for 320-slice CT scanner. Data were acquired according to a dedicated cardiac CT protocol as

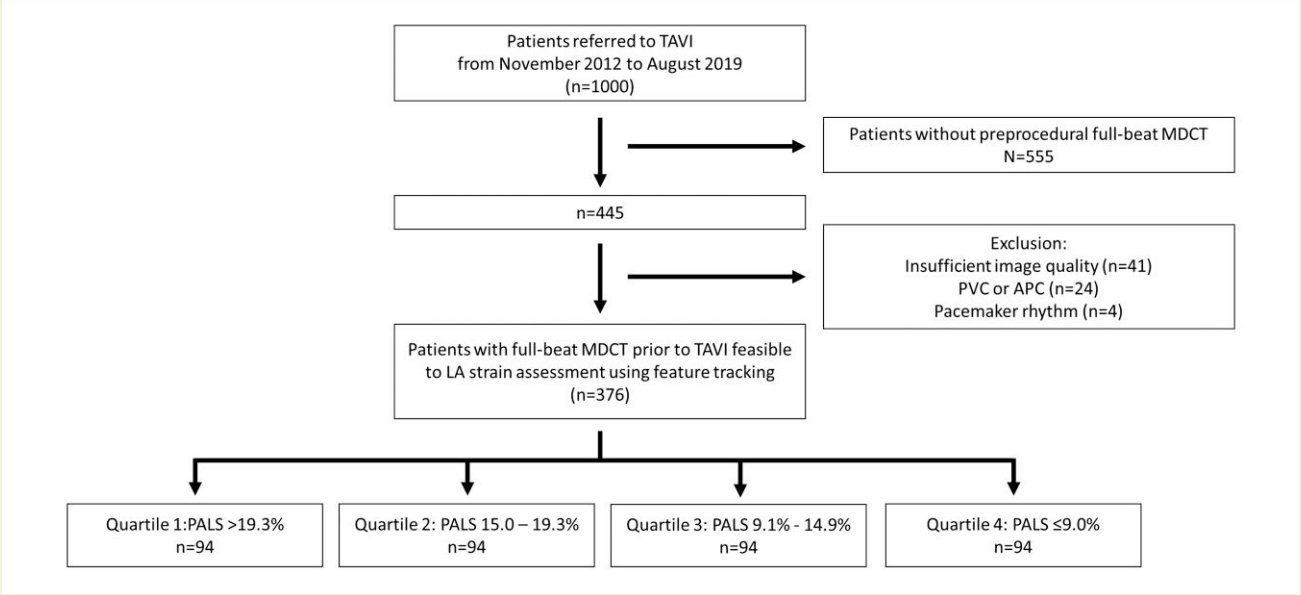

Figure 1 Study flow chart. LA, left atrium; MDCT, multi-detector computed tomography; PAC, premature atrial complex; PALS, peak left atrial longitudinal strain; PVC, premature ventricular complex; TAVI, transcatheter aortic valve implantation.

previously described.[13,14] With a 64-slice CT scanner, data acquisition was performed, gated to the electrocardiogram (ECG) to allow retrospective gating and reconstruction of the data at desired phases of the cardiac cycle (at each 10% of the RR interval and at 75–85% and 30–35% for LV end-diastole and end-systole). With a 320-slice CT scanner, prospective ECG triggered dose modulation was used. The dataset was reconstructed at each 10% of the RR-interval and transferred to a remote workstation for further offline analysis. Data processing was performed using a dedicated MDCT workstation (3mensio version 10.2, Pie Medical Imaging, Bilthoven, the Netherlands). LA volume was measured at end-systole and indexed for body surface area (BSA) (LAVI). LV end-diastolic and end-systolic volumes and ejection fraction were measured on MDCT data by tracing the endocardial and epicardial border on stacks of short-axis encompassing the entire LV. To estimate LV mass, the epi- and endocardial LV borders were manually traced at the mid-diastolic phase as previously described.[15] Subsequently, LV mass index was calculated with the following formula: LV mass index = [(LV epicardial volume – LV endocardial volume) × 1.05]/BSA. Quantification of LV GLS and PALS was performed with dedicated FT software (Medis Suite CT v3.1 Medis Medical Imaging Systems, Leiden, The Netherlands) (*Figure 2*). For LVGLS measurement, the 4-, 2-, and 3-chamber views were manually reconstructed from three-dimensional multiplanar reconstructions. Subsequently, the LV endocardial borders were manually traced in each view at end-diastole and end-systole. The FT software automatically interpolated the remaining phases and LV GLS was calculated. For PALS measurement, the two-chamber view focused on the LA was reconstructed and subsequently the LA endocardial borders were manually traced in end-diastole and end-systole with the exclusion of the LA appendage and the pulmonary veins. The remaining phases were automatically interpolated and then PALS was calculated. We previously reported good agreement between PALS assessed with FT MDCT and 2D STE using same software in a subgroup of this population (correlation coefficient = 0.789, $P < 0.001$).[9]

Transthoracic echocardiography

Comprehensive two-dimensional transthoracic echocardiography (TTE) was performed using commercially available ultrasound systems equipped with 3.5 MHz or M5S transducers (E9 or E95, GE-Vingmed, Horten, Norway) according to current guidelines.[16,17] All echocardiographic images were digitally stored on a dedicated workstation (EchoPAC Version 204, GE Medical Systems, Horten, Norway) for offline analysis. LV end-diastolic and end-systolic volumes were obtained from the apical two- and four-chamber views and subsequently the LV ejection fraction (LVEF) was calculated using the Simpson's biplane method.[17] The peak velocities of mitral inflow E and A waves were measured from the apical four-chamber view with the sample size of the pulsed wave Doppler placed at the opening of the mitral valve. The early diastolic peak velocity (e′) was measured at the septal and lateral mitral annulus in the apical four-chamber view with pulse-wave tissue Doppler imaging and averaged. Subsequently, *E*/e′ was calculated.[18] Continuous-wave Doppler was used to measure the aortic peak jet velocity in the apical three- or five-chamber views, and the transvalvular aortic gradient was assessed using the modified Bernoulli equation. The aortic valve area (AVA) was calculated using the continuity equation.[19,20] Right ventricular systolic function was assessed with the tricuspid annulus plane systolic excursion (TAPSE) measurement from M-mode of the tricuspid valve annulus on a focused right ventricular four-chamber apical view. Systolic pulmonary artery pressure was derived from the peak tricuspid regurgitant jet velocity applying the Bernoulli equation and adding 3, 8, or 15 mmHg based on inferior vena cava collapsibility.[21] The severity of tricuspid regurgitation was assessed using an integrated approach as recommended in current guidelines.[22]

Follow-up

The primary endpoint of the study was all-cause mortality after TAVI. Data on mortality were collected by review of individual patient medical records, which are linked to the governmental registry.

Figure 2 Assessment of left atrial strain using feature-tracking software. (*A*) Tracing endocardial border of the LA. (*B*) Automated calculation of left atrial strain. PALS, peak left atrial longitudinal strain.

Statistical analysis

Continuous variables are presented as mean ± standard deviation or as median and interquartile range depending on the distribution of the variables. Comparison between the groups according to PALS quartiles was performed using one-way analysis of variance and applying *post hoc* analysis with Bonferroni's correction for multiple comparisons. Categorical variables are presented as frequencies and percentages and were compared with the χ^2 or Fisher exact test as appropriate. Univariable Cox regression analysis was performed to identify the clinical and imaging variables associated with all-cause mortality. Subsequently, variables that were statistically significant in the univariable model were included in the multivariable Cox proportional hazards regression model. The hazard ratios (HRs) with 95% confidence intervals (CIs) were assessed, and the *P*-values were calculated. Kaplan–Meier curve analysis was performed to estimate the all-cause mortality rates for groups of patients based on quartiles of PALS and comparisons were performed using the log-rank test. The onset of follow-up was set at the time of the intervention. Two-sided *P*-values < 0.05 were considered statistically significant. The statistical analyses were performed using the SPSS software version 25 (SPSS, Inc., Chicago, IL, USA) and the R software (R Foundation for Statistical Computing, Vienna, Austria).

Results

Patients characteristics

A total of 376 patients (mean age 80 ± 7 years, 51% male) were included and classified into four groups according to PALS quartiles as follows: patients with PALS more than 19.3% (best LA reservoir function, Q1, *n* = 94), 15.0–19.3% (Q2, *n* = 94), 9.1–14.9% (Q3, *n* = 94), and equal to or less than 9.0% (worst LA reservoir function, Q4, *n* = 94) (*Figure 1*). Baseline demographic and clinical characteristics are shown in *Table 1*. Patients with worst LA reservoir function (Q4) had higher prevalence of atrial fibrillation, coronary artery disease and impaired kidney function, used more frequently diuretics, and underwent more often TAVI through a transapical access compared with patients with best LA reservoir function (Q1).

Imaging characteristics derived from TTE and MDCT are shown in *Table 2*. In the overall cohort, the mean LVEF was 55 ± 13%, AVA 0.76 ± 0.21 cm^2, and the mean aortic valve pressure gradient was 43 ± 17 mmHg. Mean LAVI measured with MDCT was 62 ± 19 mL/m^2. The mean FT-MDCT derived PALS and LV GLS were 14.8 ± 7.2% and 15.4 ± 4.5%, respectively. Patients with more impaired PALS had lower LVEF and lower LV GLS, smaller AVA, and lower TAPSE, compared with those with more preserved PALS. In contrast, E wave velocity, *E*/*e*′, LAVI, and systolic pulmonary arterial pressure increased across the groups, being lowest among patients in Q1 of PALS and highest among patients in Q4. Interestingly, mean aortic valve pressure gradients were comparable across groups and LV mass index was larger in the patients in Q2 compared with the other groups.

Survival analysis

During a median follow-up of 45 (22–68) months, 148 patients (39%) died. *Table 3* shows the association between clinical and imaging variables vs. all-cause mortality after TAVI.

On univariable Cox regression analysis, NYHA functional Class ≥ III, chronic obstructive pulmonary disease, coronary artery disease, transapical TAVI, use of diuretics, tricuspid regurgitation ≥ Grade 3, low estimated glomerular filtration rate, large LAVI, impaired LV GLS, and impaired PALS were significantly associated with all-cause mortality. On multivariable analysis, impaired PALS was independently associated with all-cause mortality (HR: 0.958 per 1% decrease of PALS, 95% CI: 1.326–4.335, *P* = 0.006) together with the presence of coronary artery disease, impaired renal function, and transapical TAVI. Moreover, impaired PALS (Q3 vs. Q1 and Q4 vs. Q1) were significantly associated with all-cause mortality (HR: 2.262, 95% CI:

Table 1 Baseline demographic and clinical characteristics

	All, $n = 376$	Q1, $n = 94$ (PALS > 19.3%)	Q2, $n = 94$ (PALS 15.0–19.3%)	Q3, $n = 94$ (PALS 9.1–14.9%)	Q4, $n = 94$ (PALS≤9.0%)	*P*-value
Age, years	80 ± 7	79 ± 8	79 ± 8	80 ± 7	81 ± 6	0.243
Male (%)	198 (53)	47 (50)	49 (52)	52 (55)	50 (53)	0.907
BSA, m^2	1.85 ± 0.21	1.85 ± 0.20	1.83 ± 0.20	1.87 ± 0.21	1.85 ± 0.21	0.615
NYHA class ≥ 3 (%)	219 (58)	49 (52)	52 (55)	62 (66)	56 (60)	0.246
Hypertension (%)	286 (77)	73 (78)	75 (80)	72 (77)	67 (71)	0.563
Dyslipidaemia (%)	241 (64)	63 (67)	60 (64)	62 (66)	56 (60)	0.722
Atrial fibrillation (%)	86 (23)	4 (4)	10 (11)	14 (15)	58 (62)	<0.001
COPD (%)	85 (23)	15 (16)	19 (20)	27 (29)	24 (26)	0.161
PVD (%)	116 (31)	25 (27)	29 (31)	38 (40)	24 (26)	0.108
eGFR, mL/min/m^2	61 ± 20	64 ± 19	65 ± 19	59 ± 21	56 ± 20***	0.01
Coronary artery disease (%)	229 (61)	54 (57)	59 (63)	69 (73)	47 (50)	0.009
Diabetes (%)	112 (30)	24 (26)	31 (33)	24 (26)	33 (35)	0.34
Transapical access (%)	114 (30)	15 (16)	29 (31)	40 (43)	30 (32)	0.001
Medication						
Beta-blockers (%)	237 (63)	53 (56)	56 (60)	65 (69)	63 (67)	0.22
ACE-i/ARBs (%)	198 (53)	52 (55)	47 (50)	53 (56)	46 (49)	0.664
Diuretics (%)	210 (56)	40 (43)	44 (47)	58 (62)	68 (72)	<0.001

Values are mean ± SD or *n* (%). ACE, angiotensin-converting enzyme; ARB, angiotensin II receptor blocker; BSA, body surface area; COPD, chronic obstructive pulmonary disease; eGFR, estimated glomerular filtration rate; NYHA, New York Heart Association; PALS, peak left atrial longitudinal strain; PVD, peripheral vascular disease.
*$P < 0.05$ vs. Q1.
**$P < 0.05$ vs. Q2.

Table 2 Echocardiography and multi-detector computed tomography analysis

	All, $n = 376$	Q1, $n = 94$ (PALS > 19.3%)	Q2, $n = 94$ (PALS 15.0–19.3%)	Q3, $n = 94$ (PALS 9.1–14.9%)	Q4, $n = 94$ (PALS ≤ 9.0%)	*P*-value
Echocardiographic measurement						
LVEF, %	55 ± 13	61 ± 11	57 ± 12	53 ± 14*	50 ± 14***	<0.001
AVA, cm^2	0.76 ± 0.21	0.79 ± 0.22	0.77 ± 0.19	0.77 ± 0.20	0.70 ± 0.22*	0.012
Mean AV PG, mmHg	43 ± 17	43 ± 19	46 ± 16	40 ± 15	43 ± 18	0.083
E wave velocity, mm/s	87 ± 32	73 ± 24	81 ± 31	86 ± 31*	106 ± 32*****	<0.001
E′, mm	4.8 ± 2.0	4.9 ± 1.8	4.6 ± 2.0	4.6 ± 2.0	5.2 ± 2.1	0.16
E/E′	21 ± 13	17 ± 8	21 ± 14	21 ± 11*	25 ± 15*	<0.001
TAPSE, mm	18 ± 4	19 ± 4	19 ± 5	18 ± 4	16 ± 4******	<0.001
SPAP, mmHg	35 ± 13	31 ± 10	35 ± 11	36 ± 12	40 ± 16*	<0.001
CT measurement						
LVEDV, mL	161 ± 53	148 ± 42	161 ± 47	172 ± 59*	164 ± 59	0.021
LVESV, mL	78 ± 49	60 ± 32	72 ± 41	87 ± 55*	92 ± 59***	<0.001
LVEF, %	54 ± 15	61 ± 12	57 ± 14	52 ± 15***	47 ± 16***	<0.001
LV mass index, g/m^2	91 ± 23	85 ± 19	94 ± 23*	92 ± 25	92 ± 24	0.035
LAVI, mL/m^2	62 ± 19	51 ± 11	58 ± 13	63 ± 14*	76 ± 26*****	<0.001
PALS, %	14.8 ± 7.2	24 ± 4	17 ± 11	12 ± 2***	6 ± 2*****	<0.001
LVGLS (%)	15.4 ± 4.5	17.7 ± 3.7	16.0 ± 4.1*	14.6 ± 4.4*	13.0 ± 4.6***	<0.001

Values are mean ± SD or *n* (%). AVA, aortic valve area; CT, computed tomography; LAVI, left atrial volume index; LVEF, left ventricular ejection fraction; LVGLS, left ventricular global longitudinal strain; PALS, peak left atrial longitudinal strain; SPAP, systolic pulmonary artery pressure; TAPSE, tricuspid annular plane systolic excursion.
*$P < 0.05$ vs. Q1.
**$P < 0.05$ vs. Q2.
***$P < 0.05$ vs. Q3.

Table 3 Cox regression analysis for all-cause mortality

Variables	Univariable		Multivariable	
	Hazard ratio (95% CI)	*P*-value	Hazard ratio (95% CI)	*P*-value
Clinical variables				
Age, per 1-year increase	0.979 (0.958–1.001)	0.066		
Male, yes/no	1.328 (0.958–1.839)	0.088		
NYHA class ≥3, yes/no	1.498 (1.069–2.100)	0.019	1.411 (0.998–1.994)	0.051
COPD, yes/no	1.527 (1.065–2.190)	0.021	1.382 (0.949–2.014)	0.092
CAD, yes/no	1.420 (1.006–2.006)	0.046	1.453 (1.020–2.014)	0.039
eGFR, per 1 mL/min/m^2 increase	0.983 (0.975–0.991)	<0.001	0.987 (0.978–0.996)	0.004
Diuretics, yes/no	1.453 (1.035–2.040)	0.031	0.839 (0.571–1.233)	0.371
Transapical TAVI, yes/no	1.777 (1.282–2.463)	0.001	1.755 (1.248–2.468)	0.001
AF yes/no	1.400 (0.964–2.033)	0.077		
Echocardiographic variables				
LVEF, per 1% increase	0.992 (0.981–1.003)	0.167		
AVA, per 1 cm^2 increase	1.114 (0.511–2.427)	0.786		
E/*e*′, per 1 unit increase	1.005 (0.993–1.016)	0.414		
TAPSE, per 1 mm increase	0.984 (0.946–1.023)	0.420		
SPAP, per 1 mmHg increase	1.003 (0.990–1.017)	0.619		
TR ≥3, yes/no	1.766 (1.206–2.585)	0.003	1.488 (0.973–2.274)	0.067
CT measurements				
LAVI, per 1 mL/m^2 increase	1.007 (1.000–1.014)	0.043	1.000 (0.990–1.009)	0.948
LV mass index, per 1 g/m^2 increase	1.002 (0.995–1.009)	0.532		
LVGLS, per 1% decrease	1.058 (1.022–1.096)	0.002	1.021 (0.982–1.061)	0.302
PALS by FT MDCT, per 1% decrease	0.946 (0.923–0.970)	<0.001	0.958 (1.326–4.335)	0.006
PALS Q2 vs. Q1	1.394 (0.787–2.467)	0.255		
PALS Q3 vs. Q1	2.262 (1.335–3.832)	0.002		
PALS Q4 vs. Q1	3.116 (1.864–5.210)	<0.001		

AF, atrial fibrillation; AVA, aortic valve area; CAD, coronary artery disease; CI, confidence interval; COPD, chronic obstructive pulmonary disease; CT, computed tomography; LAVI, left atrial volume index; LVEF, left ventricular ejection fraction; LVGLS, left ventricular global longitudinal strain; NYHA, New York Heart Association; PALS, peak left atrial longitudinal strain; SPAP, systolic pulmonary artery pressure; TAVI, transcatheter aortic valve implantation; TAPSE, tricuspid annular plane systolic excursion; TR, tricuspid regurgitation.

1.335–3.832, $P = 0.002$; HR: 3.116, 95% CI: 1.864–5.210, $P < 0.001$, respectively). Spline curve analysis was performed to investigate the association between PALS and all-cause mortality (*Figure 3*). Following a plateau phase for more preserved values of PALS, there was a continuous increase in HR of all-cause mortality for values of PALS below 22%. Kaplan–Meier curves showed that patients with more impaired PALS had worse outcomes compared with the group with the most preserved PALS (χ^2: 31.039, $P < 0.001$, *Figure 4*).

A sensitivity analysis was performed including only the patients who underwent 320-slice MDCT ($n = 358$). Baseline clinical, echocardiographic, and MDCT characteristics followed a similar distribution to those of the overall population (Supplementary data online, *Tables S1 and S2*): patients in Q4 (worst PALS) had more often chronic obstructive pulmonary disease, significantly worse renal function, and received more often diuretic treatment. Patients in Q3 had the highest frequency of coronary artery disease and underwent more often transapical TAVI. Patients in Q4 had worse LV systolic function, more severe AS, worse right ventricular systolic function, and higher systolic pulmonary artery pressure. The survival analysis showed that patients in Q4 had the highest cumulative all-cause mortality rates followed by patients in Q3 (Supplementary data online, *Figure S1*).

Discussion

The main findings of the present study are as follows: (i) in the cohort of patients with severe AS who underwent TAVI, those with more impaired pre-procedural PALS measured with FT MDCT had more comorbidities, more impaired LV systolic and diastolic function, and the procedure was more frequently performed through a transapical approach as compared with patients with more preserved PALS; and (ii) impaired pre-procedural FT MDCT PALS was independently associated with higher mortality rates after TAVI (*Graphical Abstract*).

The LA in severe AS

The pressure overload imposed by severe AS leads to LV hypertrophy and LV diastolic dysfunction, as well as LA dilation and LA

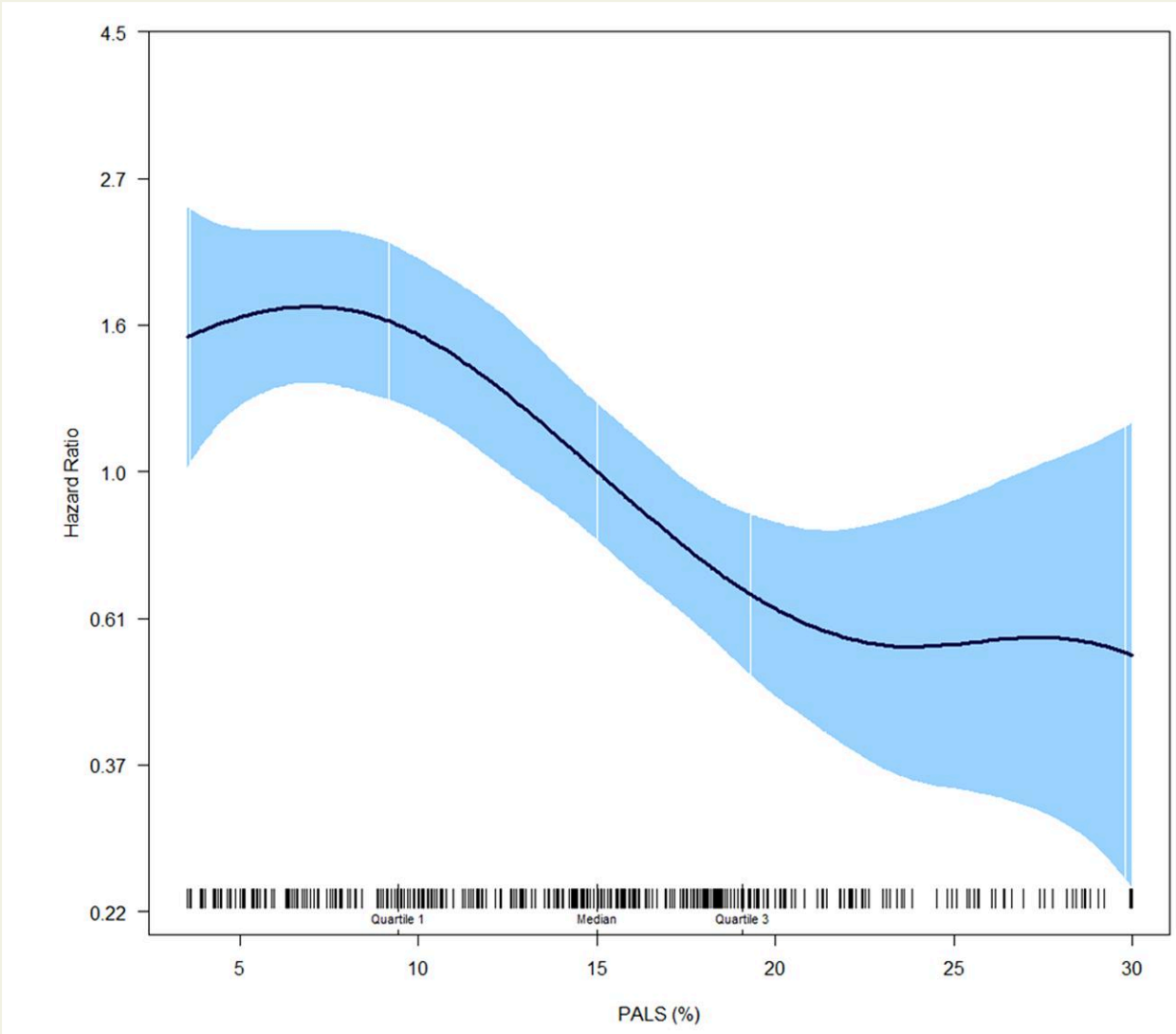

Figure 3 Spline curve analysis for all-cause mortality according to PALS. PALS, peak left atrial longitudinal strain.

dysfunction. Several studies have shown the impairment in LA reservoir function measured with STE in patients with severe AS. O'Connor *et al.*[23] demonstrated in 52 patients with severe AS, that PALS was significantly impaired as compared with individuals without AS, and that elevated LV filling pressures were the main determinants of impaired PALS. Of note, O'Connor *et al.* measured PALS based on tissue Doppler imaging-derived strain, which is influenced by the insonation angle and extrapolates the value of strain measured in one region to the entire LA. In contrast, in the present study, PALS was measured with FT MDCT, allowing assessment of PALS from the entire LA and avoiding the limitations of two-dimensional echocardiography. MDCT provides high-spatial resolution three-dimensional data allowing the reconstruction of the LA to accurately measure the volume avoiding foreshortening (as compared with two-dimensional echocardiography). In addition, the endocardial border of the LA can be accurately determined and tracked throughout the entire cardiac cycle allowing the measurement of myocardial displacement and shortening with FT MDCT. This analysis can be performed off line together with the measurement of the LV dimensions and function, assessment of the aortic annulus size, calcification burden of the aortic valve, and anatomy of the femoral arteries (key information in the TAVI planning) providing an holistic evaluation of patients with severe AS undergoing TAVI.

Prognostic value of PALS using FT MDCT in patients treated with TAVI

The prognostic value of PALS has been demonstrated in patients with severe AS. Galli *et al.*[5] showed that a value of PALS <21% measured with STE was significantly associated with major adverse cardiac events in 128 patients with severe AS. The present study confirms those results by measuring PALS with MDCT an important imaging tool to evaluate patients with severe AS who are referred to TAVI. The underlying pathophysiology explaining the association between impaired PALS and worse outcomes may be related to the

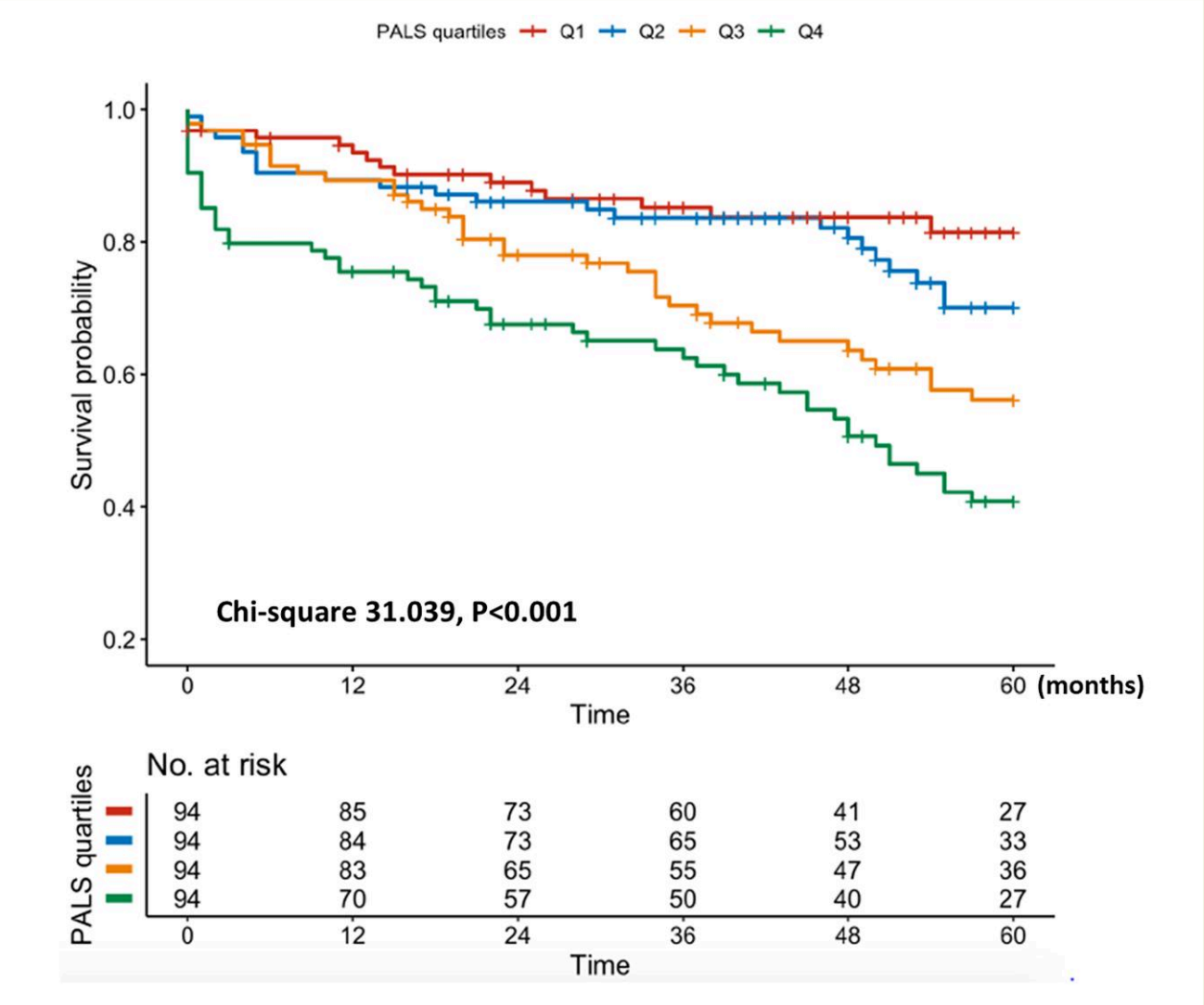

Figure 4 Kaplan–Meier analysis for all-cause mortality according to PALS quartiles. PALS, peak left atrial longitudinal strain.

fact that impaired PALS reflects impaired LA reservoir function, transmitting the increased LV filling pressures to the pulmonary vasculature, leading to pulmonary hypertension, tricuspid regurgitation, and eventually right ventricular failure. A classification algorithm based on the number of extra-aortic valve abnormalities observed on MDCT in 405 patients with severe AS who underwent TAVI has shown that the presence of LA dilation is associated with increased mortality as compared with patients who do have a normal LA size.[15] Of note, the results of the present study suggest that patients in Q3 of PALS had a higher prevalence of LV damage (reduced LVEF, LV GLS, and diastolic dysfunction) while patients in Q4 of PALS had also right heart abnormalities, which were associated with increased mortality risk. Accordingly, PALS measured with FT MDCT may provide further insights into LA damage for risk stratification after TAVI. Besides, the results suggest that the optimal cut-off values for PALS measured by FT MDCT may be lower compared with PALS measured by STE, which has been reported in a previous study.[5] These observations might be helpful for decision-making in patients with severe AS who are referred to TAVI.

Study limitations

Several limitations of the present study should be acknowledged. First, this single-centre study had limitations inherent to the retrospective observational study design. Second, LA strain measurement was only applied to patients with good contrast-enhanced MDCT image quality and this may represent a source of selection bias. Third, the FT MDCT software only supports LA strain assessment derived from a two-chamber view due to a technical reason. The software traces the border of the LA endocardium and the contrast in LA. The interatrial septum is a thin structure and not technically feasible to trace on FT MDCT data. Therefore, the two-chamber view was used for FT MDCT derived LA strain analysis in the present study. Nevertheless, the possibility to reconstruct the two-chamber LA view without foreshortening represents an advantage compared with two-dimensional echocardiography speckle tracking. Fourth, in contrast to echocardiographic strain analysis, which can be performed from multiple beat acquisition in patients, with atrial fibrillation, the measurement of PALS with FT-MDCT was performed from MDCT data acquired in only one cardiac cycle, since the acquisition

across multiple beats will incur in high radiation dose. However, the MDCT data acquisition was performed when the R–R intervals were stable and slow enough to allow subsequent reproducible analyses of PALS with FT-MDCT from one single beat.[9] Fifth, the primary endpoint was all-cause mortality since the cause of death was not systematically available in all patients.

Conclusion

Impaired PALS measured with FT MDCT is independently associated with increased all-cause mortality after TAVI.

Supplementary material

Supplementary material is available at *European Heart Journal – Cardiovascular Imaging* online.

Funding

K.H. is financially supported by an European Society of Cardiology research grant (R-2018-18122).

Disclosures

The Department of Cardiology of the Leiden University Medical Center received research grants from Abbott Vascular, Bayer, Bioventrix, Medtronic, Biotronik, Boston Scientific, GE Healthcare, and Edwards Lifesciences. N.A.M. and J.J.B. received speaker fees from Abbott Vascular. V.D. received speaker fees from Abbott Vascular, Edwards Lifesciences, GE Healthcare, MSD, and Medtronic. The remaining authors have nothing to disclose.

Data availability

The data underlying this article will be shared on reasonable request to the corresponding author.

References

1. Carluccio E, Biagioli P, Mengoni A, Francesca Cerasa M, Lauciello R, Zuchi C *et al.* Left atrial reservoir function and outcome in heart failure with reduced ejection fraction. *Circ Cardiovasc Imaging* 2018;**11**:e007696.
2. Freed BH, Daruwalla V, Cheng JY, Aguilar FG, Beussink L, Choi A *et al.* Prognostic utility and clinical significance of cardiac mechanics in heart failure with preserved ejection fraction: importance of left atrial strain. *Circ Cardiovasc Imaging* 2016;**9**:e003754.
3. Mandoli GE, Pastore MC, Benfari G, Bisleri G, Maccherini M, Lisi G *et al.* Left atrial strain as a pre-operative prognostic marker for patients with severe mitral regurgitation. *Int J Cardiol* 2021;**324**:139–45.
4. Khan MS, Memon MM, Murad MH, Vaduganathan M, Greene SJ, Hall M *et al.* Left atrial function in heart failure with preserved ejection fraction: a systematic review and meta-analysis. *Eur J Heart Fail* 2020;**22**:472–85.
5. Galli E, Fournet M, Chabanne C, Lelong B, Leguerrier A, Flecher E *et al.* Prognostic value of left atrial reservoir function in patients with severe aortic stenosis: a 2D speckle-tracking echocardiographic study. *Eur Heart J Cardiovasc Imaging* 2016;**17**:533–41.
6. Mateescu AD, Călin A, Beladan CC, Roşca M, Enache R, Băicuş C *et al.* Left atrial dysfunction as an independent correlate of heart failure symptoms in patients with severe aortic stenosis and preserved left ventricular ejection fraction. *J Am Soc Echocardiogr* 2019;**32**:257–66.
7. Meimoun P, Djebali M, Botoro T, Djou Md U, Bidounga H, Elmkies F *et al.* Left atrial strain and distensibility in relation to left ventricular dysfunction and prognosis in aortic stenosis. *Echocardiography* 2019;**36**:469–77.
8. Szilveszter B, Nagy AI, Vattay B, Apor A, Kolossváry M, Bartykowszki A *et al.* Left ventricular and atrial strain imaging with cardiac computed tomography: validation against echocardiography. *J Cardiovasc Comput Tomogr* 2020;**14**:363–9.
9. Hirasawa K, Kuneman JH, Singh GK, Gegenava T, Hautemann D, Reiber JHC *et al.* Comparison of left atrial strain measured by feature tracking computed tomography and speckle tracking echocardiography in patients with aortic stenosis. *Eur Heart J Cardiovasc Imaging* 2021;**23**:95–101.
10. Gegenava T, Vollema EM, Abou R, Goedemans L, van Rosendael A, van der Kley F *et al.* Prognostic value of thoracic aorta calcification burden in patients treated with TAVR. *JACC Cardiovas Imaging* 2019;**12**:216–7.
11. Fukui M, Xu J, Thoma F, Sultan I, Mulukutla S, Elzomor H *et al.* Baseline global longitudinal strain by computed tomography is associated with post transcatheter aortic valve replacement outcomes. *J Cardiovasc Comput Tomogr* 2020;**14**:233–9.
12. Gegenava T, van der Bijl P, Hirasawa K, Vollema EM, van Rosendael A, van der Kley F *et al.* Feature tracking computed tomography-derived left ventricular global longitudinal strain in patients with aortic stenosis: a comparative analysis with echocardiographic measurements. *J Cardiovasc Comput Tomogr* 2020;**14**:240–5.
13. van Rosendael PJ, Joyce E, Katsanos S, Debonnaire P, Kamperidis V, van der Kley F *et al.* Tricuspid valve remodelling in functional tricuspid regurgitation: multidetector row computed tomography insights. *Eur Heart J Cardiovasc Imaging* 2016;**17**:96–105.
14. van Velzen JE, Schuijf JD, de Graaf FR, Boersma E, Pundziute G, Spano F *et al.* Diagnostic performance of non-invasive multidetector computed tomography coronary angiography to detect coronary artery disease using different endpoints: detection of significant stenosis vs. detection of atherosclerosis. *Eur Heart J* 2011;**32**:637–45.
15. Hirasawa K, van Rosendael PJ, Fortuni F, Singh GK, Kuneman JH, Vollema EM *et al.* Prognostic implications of cardiac damage classification based on computed tomography in severe aortic stenosis. *Eur Heart J Cardiovasc Imaging* 2022;**23**:578–85.
16. Lancellotti P, Tribouilloy C, Hagendorff A, Popescu BA, Edvardsen T, Pierard LA *et al.* Recommendations for the echocardiographic assessment of native valvular regurgitation: an executive summary from the European association of cardiovascular imaging. *Eur Heart J Cardiovasc Imaging* 2013;**14**:611–44.
17. Lang RM, Badano LP, Mor-Avi V, Afilalo J, Armstrong A, Ernande L *et al.* Recommendations for cardiac chamber quantification by echocardiography in adults: an update from the American society of echocardiography and the European association of cardiovascular imaging. *J Am Soc Echocardiogr* 2015;**28**:1–39.e14.
18. Nagueh SF, Smiseth OA, Appleton CP, Byrd BF 3rd, Dokainish H, Edvardsen T *et al.* Recommendations for the evaluation of left ventricular diastolic function by echocardiography: an update from the American society of echocardiography and the European association of cardiovascular imaging. *J Am Soc Echocardiogr* 2016;**29**:277–314.
19. Baumgartner HC, Hung JC-C, Bermejo J, Chambers JB, Edvardsen T, Goldstein S *et al.* Recommendations on the echocardiographic assessment of aortic valve stenosis: a focused update from the European association of cardiovascular imaging and the American society of echocardiography. *Eur Heart J Cardiovasc Imaging* 2017;**18**:254–75.
20. Baumgartner H, Hung J, Bermejo J, Chambers JB, Edvardsen T, Goldstein S *et al.* Recommendations on the echocardiographic assessment of aortic valve stenosis: a focused update from the European association of cardiovascular imaging and the American society of echocardiography. *J Am Soc Echocardiogr* 2017;**30**:372–92.
21. Rudski LG, Lai WW, Afilalo J, Hua L, Handschumacher MD, Chandrasekaran K *et al.* Guidelines for the echocardiographic assessment of the right heart in adults: a report from the American society of echocardiography endorsed by the European association of echocardiography, a registered branch of the European society of cardiology, and the Canadian society of echocardiography. *J Am Soc Echocardiogr* 2010;**23**:685–713; quiz 786–8.
22. Topilsky Y, Maltais S, Medina Inojosa J, Oguz D, Michelena H, Maalouf J *et al.* Burden of tricuspid regurgitation in patients diagnosed in the community setting. *JACC Cardiovas Imaging* 2019;**12**:433–42.
23. O'Connor K, Magne J, Rosca M, Piérard LA, Lancellotti P. Impact of aortic valve stenosis on left atrial phasic function. *Am J Cardiol* 2010;**106**:1157–62.